Whole-body Motion Planning

Eiichi Yoshida, Fumio Kanehiro and Jean-Paul Laumond

Abstract This chapter addresses whole-body motion planning for humanoid robots. Taking advantage of recent progress of motion planning techniques for many degrees of freedom (DOF) systems, early work in humanoid motion planning started with a two-stage approach that utilizes kinematic and geometric motion planning to plan a rough path that is later transformed into a whole-body motion including locomotion with a dynamic biped walking pattern generator. Subsequent progress beyond this functional decomposition is to exploit all the DOFs for the desired task. Whole-body motion planning was then tackled by integrating generalized inverse kinematics that allows achieving the specified tasks by taking into account such constraints as balance, foot positions or joint limits at the same time. Some applications are presented such as reactive planning in changing cluttered environments, whole-body manipulation of bulky objects, and footstep planning by variable kinematic modeling of footholds. The effectiveness of the proposed methods have been validated through experiments with the human-size humanoid platform HRP-2.

Key words: Humanoid, Motion Planning, Whole-body Control, Generalized Inverse Kinematics, Manipulation, Footstep Planning

1 Introduction

This chapter outlines research work on whole-body motion planning for humanoids. During 1990's, sampling-based motion planning methods exhibited notable progress

E. Yoshida, F. Kanehiro
CNRS-AIST JRL (Joint Robotics Laboratory), UMI3218/RL, Tsukuba Central 1, 1-1-1 Umezono, Tsukuba, Ibaraki 305-8560 Japan e-mail: {e.yoshida,f-kanehiro}@aist.go.jp
J.-P. Laumond,
LAAS-CNRS, 7 avenue du Colonel Roche, F-31077 Toulouse, and Universite de Toulouse ; F-31077 Toulouse, France. e-mail: jpl@laas.fr

in their theory and applications [28, 4]. This approach is represented by diffusing methods like Rapidly-exploring Random Trees (RRT) [15, 30] and sampling methods like Probabilistic RoadMap (PRM) [24] and many of their variants have been proposed. This planning technique allows dealing with many degrees of freedom (DOFs) by efficiently sampling configurations and searching a collision-free path connecting them from the start to the goal. From early 2000's [25], sampling-based motion planning started being applied to humanoid robots whose configuration space is composed joint angles and their base position usually set at the pelvis. Research in whole-body motion planning has been enjoying a rapid growth along with the continuous progress of sampling-based methods that has affinity with problems with many DOFs. At the same time, motion planning was used to generate the movement of animation characters in computer graphics[9].

Early studies in humanoid motion planning started with a two-stage approach that utilizes kinematic and geometric motion planning to plan a rough path that is later transformed into a whole-body motion including locomotion with a dynamic biped walking pattern generator [51]. The upper-body motion was considered as disturbance for biped locomotion that is adapted to maintain the dynamic stability. This first approach was based on functional decomposition that assigns manipulation and locomotion to upper and lower bodies respectively [42, 9]. However, observing us humans, when we do some tasks with hands and arms, we use our lower body to generate smooth and efficient motions.

The subsequent progress beyond this functional decomposition is to exploit all the DOFs for the desired task. Whole-body motion planning was then tackled by generalized inverse kinematics [43, 33] that allows achieving the specified tasks by taking into account such constraints as balance, foot positions or joint limits at the same time. The main particularities of humanoid robot from the viewpoint of inverse kinematics are the following: necessity of dynamic balancing, a floating base frame, and changing support foot on the ground [53]. Utilization of generalized inverse kinematics for humanoid whole-body motion planning and generation lead to a variety of applications such as locomotion planning, manipulation and reactive behaviors. This chapter finally presents future issues of integration of dynamics in whole-body motion planning.

2 Humanoids Meets Planning - Walking and Manipulation

Especially after the appearance of P2 of Honda [14], biped locomotion technology for human-size humanoids made a remarkable progress. One of the methods for biped walking pattern generation that became a de facto standard is zero moment point (ZMP) based preview control [16]. Based on an invert pendulum model describing the relationship between the ZMP and the Center of Mass (COM), the control framework generates the reference velocity of the COM from the desired footsteps that correspond to the ZMP trajectory. A biped walking motion of both legs can then be computed using swing foot trajectory.

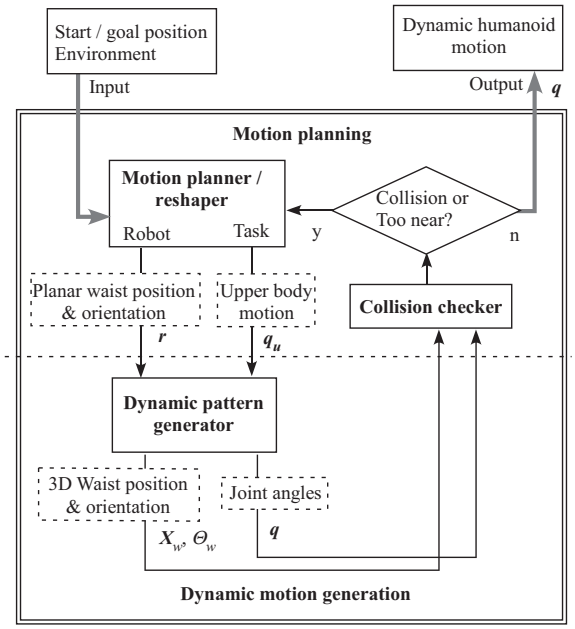

Fig. 1 Two-stage motion planning framework. Based on kinematic and geometric motion planning, the first stage generates a collision-free path that is later converted into dynamic motion in the second stage. If collisions are detected the path is sent back to the first stage. This process is repeated until a collision-free dynamic trajectory is obtained.

The research on this walking walking pattern generator focused on biped locomotion. Next step is combination with complex upper body motions like manipulation or collision avoidance during walking. In order to allow manipulation during locomotion, a general and practical iterative two-stage planning framework has been proposed that integrates a geometric path planner and a dynamic motion generator [51]. In this chapter, an off-line method is presented under the assumption that the environment is fully known in advance. Static constraints such as joint limits can be incorporated whereas the dynamics is taken into account by the dynamic motion generator.

The first stage generates a geometric and kinematic "path" connecting feasible configurations, which is transformed into a "trajectory" along the time through appropriate dynamic motion generators in the second stage. Dynamic effects may cause difference between the initial path and the new trajectory. Then the output trajectory is again verified with respect to the collision avoidance by the first stage and reshaped if necessary. This process is iterated until a valid dynamic trajectory is obtained as illustrated in Fig. 1.

This iterative method is inspired by a technique for key frame editing in the context of computer animation [10]. This approach places more emphasis on the gradual transition from the colliding trajectory by maintaining the motion timing in constrained environments. Another feature of this approach is the practical aspect of implementation that is advantageous for realistic simulations and experiments.

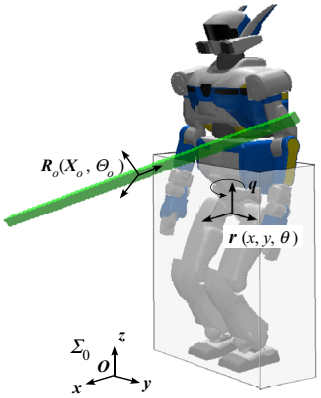

Fig. 2 Humanoid modeled by rectangle box with a bar. In the first stage the geometric and kinematic path planner generates collision-free path for the 9 DOF system including robot waist ($\boldsymbol{r}$, 3DOF) and object ($\boldsymbol{R}_o$, 6DOF).

2.1 First Stage: Geometric and Kinematic Path Planning

The path planner finds a geometric and kinematic collision-free path in 3D at the first stage (upper part of Fig. 1) where the robot is modeled as a geometric bounding box (Fig. 2). Collision-free path is planned for that box and the manipulated object. The robot motion is expressed by the planar position and orientation of its waist $\boldsymbol{r}(x, y, \theta)$ (3 DOFs) and the object motion by its position and orientation $\boldsymbol{R}_o(\boldsymbol{X}_o, \boldsymbol{\Theta}_o)$ (6 DOFs) with respect to a global coordinate system Σ_0. As a result, the configuration space to be searched has 9 dimensions.

Note that any available planning method can be used for this part. In the present humanoid motion planning, the robot path is planned with PRM using Dubins curves composed of line segments and arcs of a circle [7] as its local method connecting sampled configurations. Given the configuration of the robot waist and object, the joint angles ($\boldsymbol{q}_u$) of the upper-body motion are derived by using inverse kinematics described later.

2.2 Second Stage: Dynamic Motion and Smooth Path Reshaping

In the second stage, the dynamic motion generator to transform the given path into dynamically executable robot trajectory (lower part in Fig. 1). A dedicated dynamic controller can be integrated depending on the application. The generated trajectory may deviate from the planned path due to robot dynamics, which may cause unpredicted collision with obstacles. Those local collisions are removed by "reshaping" the original path back in the first stage.

First, the planned motions $\boldsymbol{r}$ and $\boldsymbol{q}_u$ are given to the dynamic pattern generator such as [16] of humanoid robots to transform the input planar path into a dynamically stable biped walking motion that always maintains the ZMP inside the support

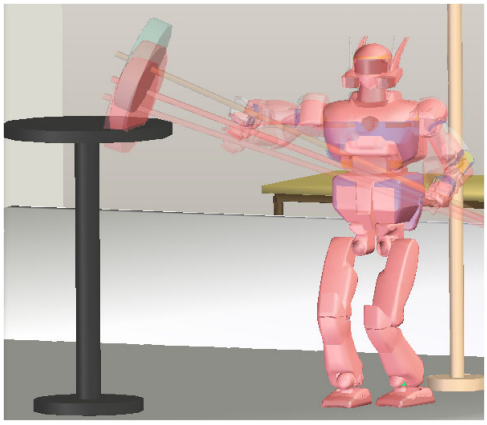

Fig. 3 Transition of robot configurations during the reshaping. The colliding part of the carried object goes away from the obstacle by increasing tolerance.

polygon formed by the foot (feet). Moreover, the pattern generator can combine upper-body motion $\boldsymbol{q}_u$ as auxiliary input to compute the mixed whole-body motion. Finally, the dynamic whole-body humanoid motion is computed as the 6 DOF waist position and orientation $\boldsymbol{R}_w(\boldsymbol{X}_w, \boldsymbol{\Theta}_w)$ and joint angles of whole body ($\boldsymbol{q}$).

If collisions are found within the upper part of the body, the following reshaping procedure is applied. One practical implementation is to locally deform the colliding part of the path by "growing" the obstacles for the robot to move away from the obstacles. If the dynamically colliding local paths become blocked by the "grown" obstacles, a replanning process is activated. After identifying the endpoints each colliding portion, the path planner searches for another path that avoids the blocked passage. Inverse kinematics (IK) is then applied to satisfy the constraints of the hands at each sample of the reshaped trajectory that synchronizes the upper body task with the lower body motion. As a result, this reshaping eliminates the collision locally as shown in Fig. 3.

The proposed method is implemented as an off-line planner and applied to a task of carrying a bulky object in an environment with several obstacles. Figure 4 shows the experimental results of the planned motion.

Since the distance between the two lamps is shorter than the bar length, the bar should pass through with an angle. At the beginning of the motion, the computed trajectory for the bar makes the robot move to the left, then walk forward with a certain angle to path through the gap (Fig. 4a,b). Here the motion of the upper body of the robot is computed using a generalized inverse kinematics whose root is the chest that is moved consequently to complete both tasks.

This example also shows that the complete 3D geometry of the object has been exploited for collision avoidance (Fig. 4d) where the concave part of the disk and the bar is close to the lamp.

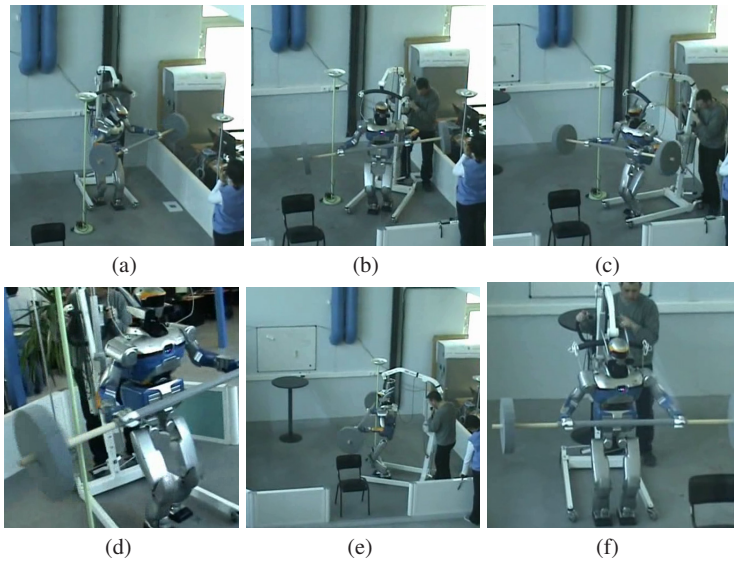

Fig. 4 Experiment of 3D collision-free motion for bar-carrying task at JRL-France

3 Whole-body Motion Planning with Generalized Inverse Kinematics

In the previous section, the roles of lower and upper body was assigned in a distinct manner, for walking and manipulation respectively. This idea comes from a functional decomposition of virtual mannequins with redundant DOFs shown in [9].

This section takes a step forward in order to generate automatically the motion to achieve the desired tasks through whole-body motion, by taking into account such constraints as balance, foot positions or joint limits at the same time. Generalized inverse kinematics technique with task priority and its extension [43, 33] is utilized as a key tool for local whole-body motion generation.

The main particularities of humanoid robot from the viewpoint of inverse kinematics are the following: necessity of dynamic balancing, a floating base frame, and changing ground support during walking. Those issues are also regarded as generalized tasks and integrated in a unified framework of generalized inverse kinematics by taking into account their priorities. We will also mention incorporation of inequality constraints with priorities in the same framework.

This local motion resolution based on generalized inverse kinematics is then combined with global motion planning algorithms in order to generate the whole-body motions to accomplished the desired tasks. The sampling-based method presented in 1 can again be used to search a global path composed of configurations to the goal, while the generalized inverse kinematics framework generates the local whole-body motions connecting them. Since the method is local, it can be ap-

plied to partially known or dynamic environments together with appropriate planning techniques. Kinematic robot constraints including inequalities such as joint limits, stability conditions, or preferred end-effector regions can also be handled in this framework.

3.1 Task-driven Local Whole-body Motion Generation

Intensive studies have been made on whole-body motion generation to achieve given tasks. Khatib and his colleagues have been working on dynamic motion generation for humanoid robots by using task specification in operational space approach [41]. In their work a hierarchical controller synthesizes whole-body motion based on prioritized behavioral primitives including postures and other tasks in a reactive manner. Kajita et al. proposed a "resolved momentum control" to achieve specified momentum by whole-body motion [17]. Mansard et al. [31] proposed a task sequencing scheme to achieve several tasks including walking and reaching at the same time.

In this section, we introduce a general method for whole-body motion generation including stepping and tasks in the workspace, such as reaching or manipulation. Figure 5 illustrates the proposed method with an example of a reaching task [53]. Priorities are given to the target task as well as to other tasks such as the position of COM. We employ generalized inverse kinematics to generate a whole-body motion

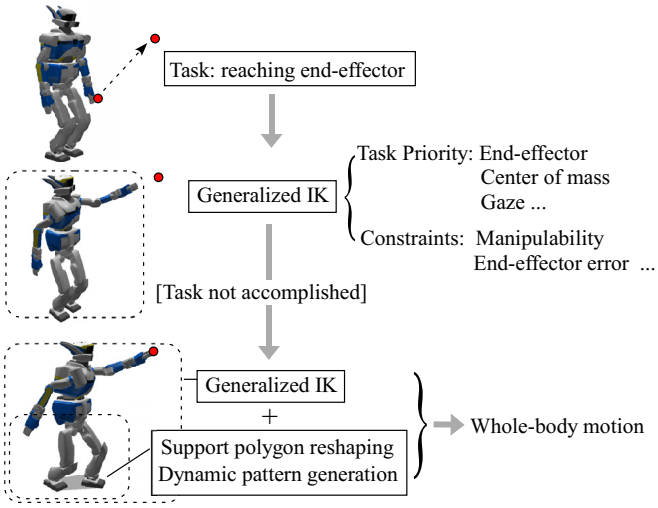

Fig. 5 A general framework for task-driven whole-body motion including simultaneous reaching and stepping [53]. If the desired tasks cannot be achieved, stepping motion is generated to increase the workspace.

for those tasks based on the given priorities [33]. During the motion, several constraints are monitored which are expressed by such measures as manipulability for whole-body, end-effector errors from target, or joint limits.

If the task cannot be achieved because those monitored constraints are not satisfied, a reshaping planner of support polygon is activated automatically to increase accessible space of the robot, keeping the inverse kinematics working to achieve the tasks. The reshaping is performed based on geometric planning to deform the support polygon in the direction required by the specified task. Thanks to the usage of free-floating base, the changes in support phase can be easily integrated in the computation. As a result, the stepping motion is generated using a biped walking pattern generator [16] and the blended whole-body motion including the target task is recalculated.

Let us consider a task $\dot{\boldsymbol{x}}_j$ with priority j in the workspace and the relationship between the joint angle velocity $\dot{\boldsymbol{q}}$ is described using Jacobian matrix, like

$$\dot{\boldsymbol{x}}_j = \boldsymbol{J}_j \dot{\boldsymbol{q}}. \tag{1}$$

For the tasks with the first priority, using pseudo-inverse $\boldsymbol{J}_1^{\#}$, the joint angles that achieves the task is given:

$$\dot{\boldsymbol{q}}_1 = \boldsymbol{J}_1^{\#} \dot{\boldsymbol{x}}_1 + (\boldsymbol{I}_n - \boldsymbol{J}_1^{\#} \boldsymbol{J}_1) \boldsymbol{y}_1 \tag{2}$$

where $\boldsymbol{y}_1$, n and $\boldsymbol{I}_n$ are an arbitrary vector, the number of the joints and identity matrix of dimension n respectively.

For the task with second priority $\dot{\boldsymbol{x}}_2$, the joint velocities $\dot{\boldsymbol{q}}_2$ is calculated as follows [33]:

$$\begin{aligned} \dot{\boldsymbol{q}}_2 &= \dot{\boldsymbol{q}}_1 + \hat{\boldsymbol{J}}_2^{\#} (\dot{\boldsymbol{x}}_2 - \boldsymbol{J}_2 \dot{\boldsymbol{q}}_1) + (\boldsymbol{I}_n - \boldsymbol{J}_1^{\#} \boldsymbol{J}_1)(\boldsymbol{I}_n - \hat{\boldsymbol{J}}_2^{\#} \hat{\boldsymbol{J}}_2) \boldsymbol{y}_2 \\ &\text{where} \quad \hat{\boldsymbol{J}}_2 \equiv \boldsymbol{J}_2 (\boldsymbol{I}_n - \boldsymbol{J}_1^{\#} \boldsymbol{J}_1) \end{aligned} \tag{3}$$

where $\boldsymbol{y}_2$ is an arbitrary vector of dimension n. It can be extended to the task of j^{th} ($j \geq 2$) priority in the following formula [1, 43].

$$\begin{aligned} \dot{\boldsymbol{q}}_j &= \dot{\boldsymbol{q}}_{j-1} + \hat{\boldsymbol{J}}_j^{\#} (\dot{\boldsymbol{x}}_j - \boldsymbol{J}_j \dot{\boldsymbol{q}}_{j-1}) + \boldsymbol{N}_j \boldsymbol{y}_j \\ \boldsymbol{N}_j &\equiv \boldsymbol{N}_{j-1} (\boldsymbol{I}_n - \hat{\boldsymbol{J}}_j^{\#} \hat{\boldsymbol{J}}_j), \; \hat{\boldsymbol{J}}_j \equiv \boldsymbol{J}_j (\boldsymbol{I}_n - \hat{\boldsymbol{J}}_{j-1}^{\#} \hat{\boldsymbol{J}}_{j-1}) \end{aligned} \tag{4}$$

While the motion is being computed by the generalized IK, several properties are monitored.

One of the important measures is the manipulability [57] defined as:

$$w \equiv \sqrt{\det\{\boldsymbol{J}\boldsymbol{J}^T\}} \tag{5}$$

This measure is continuously tracked during the motion generation as well as others such as joint angle limits or end-effector errors from the target. If it becomes below a certain value, it means that it is difficult to achieve the task.

Joint limit constraints can be taken into account by introducing a selection diagonal matrix $\boldsymbol{S} = \text{diag}\{S_1, \ldots S_n\}$ ($S_i = 0$ or 1) to be multiplied to Jacobian to select the activated joints if the corresponding joint reaches a limit angle. The selection matrix is $\boldsymbol{I}_n$ if all the joints are used to achieve the task.

When one or more monitored measures go out of the admissible range to prevent the task from being achieved, stepping motion is activated to extend the accessible space. The main idea is to step toward by a foot toward the target position projected on the ground. The new foot position is chosen in such a way that it maximizes the advance towards the target position. This simple algorithm allows the humanoid robot to make a step motion, keeping a large margin of accessible area for the task by facing the upper body to the target direction.

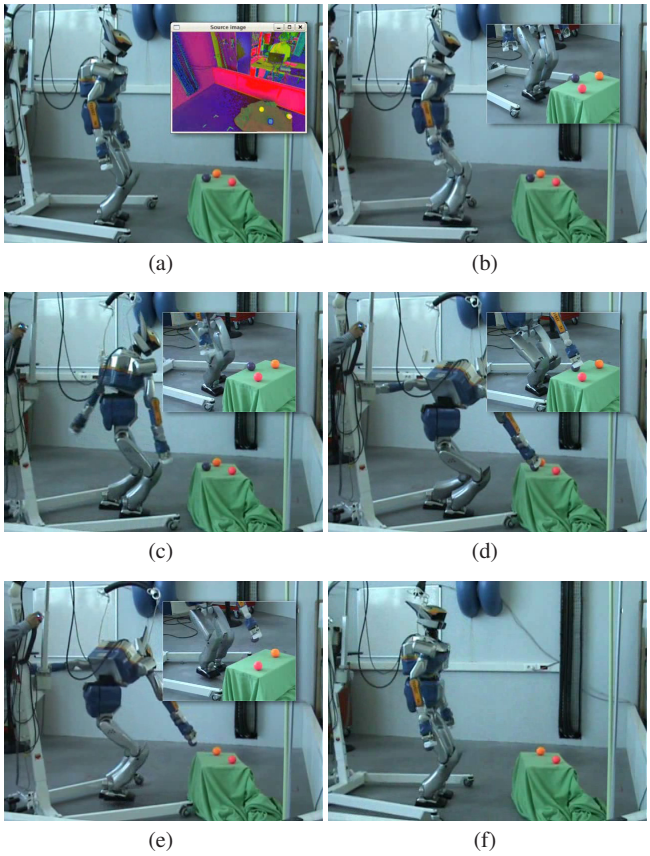

Fig. 6 A whole-body grasping motion generated through task-priority generalized inverse kinematics [53]. Upper and lower bodies coordinate to achieve the desired grasping task while making a step and maintaining the balance.

Figure 6 shows the whole-body reaching motion including a step to take a ball localized by a vision system [53]. The high priority is assigned to COM and the foot motion to avoid falling in this example. As can be seen, the legs are used not only for stepping but also bending to reach a lower position in a manner coordinated with the upper body. The left arm moves backwards as the result of balancing task. Whole-body motions for manipulation of daily-life tools [36] and also for self-collision avoidance [47] have been implemented also based on a similar framework.

The manipulability measure of the arm during the forward reaching task is provided in Fig. 7. Without stepping, the arm approaches singular configuration where the manipulability becomes lower than the threshold at 2.3[s] and the computation keeping the same support polygon is discarded. The reshaping starts at this moment to recalculate the overall whole-body motion including stepping motion. We can see the manipulability regains higher value at the final position.

So far the generalized inverse kinematics has been applied with equality tasks, for example reaching the end-effector to a desired position in the workspace. We may want to achieve tasks expressed as inequalities, like avoiding some regions or obstacles, maintaining the COM within some area, or keeping the gaze direction in some range. The generalized inverse kinematics presented so far has been extended to prioritized tasks represented as mixed equalities and inequalities [22, 21].

The key idea is to represent the relationship of velocity like Eq. (1) as a linear system. Tasks that aims at achieving a local velocity is regarded as an optimization problem. The inequality tasks can be integrated as inequalities for the quadratic programming (QP).

At the level of priority $k \in \{1, \ldots, p\}$, we consider linear equality $\boldsymbol{A_k x} = \boldsymbol{b}_k$ and inequality $\boldsymbol{C_k x} \leq \boldsymbol{d}_k$ indexed with k. At each level of priority, the following opti-

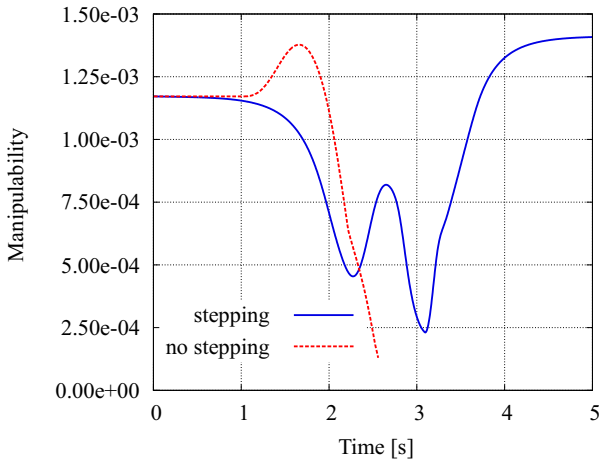

Fig. 7 Manipulability measure for reaching motion. Without stepping, the manipulability measure decreases below the threshold. Although it also decreases for stepping motion, the manipulability finally increases after stepping.

mization is performed by satisfying the sets of solutions $S_0 \ldots S_k$ with the system with higher priorities, like

$$S_{k+1} \subseteq S_k. \tag{6}$$

The quadratic programming problem can be written as follows:

$$S_0 = \Re^n, \tag{7}$$

$$S_{k+1} = \underset{x \in S_k, w \in \Re}{\text{Arg min}} \quad \frac{1}{2}||\boldsymbol{A_k x} - \boldsymbol{b}_k||^2 + \frac{1}{2}||\boldsymbol{w}^2||, \tag{8}$$

$$\text{s.t.} \quad \boldsymbol{C_k x} - \boldsymbol{w} \leq \boldsymbol{d}_k. \tag{9}$$

If S_k is a non-empty convex polytope, S_{k+1} becomes also a non-empty convex polytope that can always be represented by systems of linear equalities and inequalities. The readers are referred to the reference [21] for details. The presented framework is still local, but optimization can also be used to generate a global whole-body humanoid trajectory based on certain criteria, for total example energy consumed during the motion[49, 48]. Optimization-based trajectory generation, which is still being studied intensively, is presented in another Chapter (**??**).

Figure 8 shows a task of reaching towards the object on the floor [22]. The task with the first priority is to reach the goal, whereas the inequality constraint that requires the robot to have the visibility of the goal (green zone) as much as possible. At the beginning this inequality constraint is respected while it is violated until the end of the motion when the reaching task is achieved.

3.2 Efficient Global Motion Planning for Whole-body Humanoid Tasks

We have discussed the local whole-body motion generation for humanoid in the previous subsection. For the humanoid robot to achieve desired tasks, its motion from

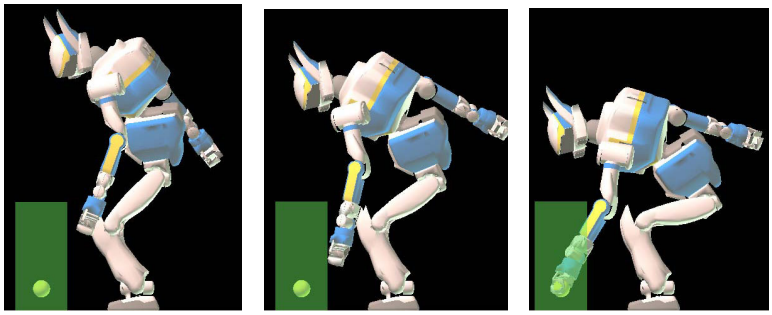

Fig. 8 Reaching task with the inequality task at lower priority.

the initial configuration to the goal should be planned appropriately. As mentioned earlier, sampling-based motion planning methods have been frequently employed for this purpose thanks to its capacity of coping with many DOFs.

Whereas the method presented in section 2 splits the DOFs into those of upper-body and lower-body to assign the roles of manipulation and walking respectively, the global motion planning here aims at exploiting all the DOFs to perform the tasks with priorities in a more flexible and efficient manner. In addition to the particularities of humanoid motion planning such as dynamic balancing, changing fixed root joint for walking and floating base frame, one important issue to is that the goal is often given in workspace, not in configuration space. Moreover, the goal might not be a single position and orientation but a manifold in 6-D space. Mainly for fixed-base or mobile manipulators, several methods have been already proposed. Weghe et al. proposed JT-RRT[50] which interleaves growing a tree randomly and growing a tree towards a goal using Jacobian transpose. An advantage of the method is an analytical solution of inverse kinematics is not required. Berenson et al. proposed IKBiRRT[3], more generalized CBiRRT2 [2] which interleaves sampling goals and growing a tree. Dalibard et al. [5] also showed whole-body humanoid motion planning method based on RRT-Connect algorithm [26] by expanding a search tree on the manifold constrained by the task in workspace. Another approach is to precompute the reachable space in advance. Zacharias et al proposed a discrete map representation of the robot arm's reachable workspace with multi-dimensional correlation. The whole-body configuration of the humanoid can be derived by referring the end-effector configuration in the map. Task-specific trajectories can also be planned by searching in the reachability map [58, 59].

We here present an efficient method for generation of whole-body reaching motion based on fast coarse planning and real-time whole-body motion execution [19]. In this work, goal configurations can be obtained by computing a configuration which corresponds to a goal sampled from a manifold called *Workspace Goal Region* using inverse kinematics. The plant environment shown in Fig. 9a is employed as an example of complex environments.

In general, time-consuming processes of the motion planning are a collision detection between the robot and the environment and a projection of a sampled configuration onto constrained manifolds. Since these processes are called many times to find an initial path and optimize it, they should be done efficiently. We adopt a collision model using sphere trees [38] and a projection that satisfies stability and kinematic constraints by maintaining approximated COM position and computing arm and leg configurations with analytical inverse kinematics.

While reaching the target, a humanoid robot must respect many constraints such as feet position/orientation and COM position. Due to high redundancy, the usual approach is to solve whole-body inverse kinematics numerically through iterative convergence computation. It is however obvious that analytical solutions of inverse kinematics should be used for quick planning.

The reaching task can be naturally defined by a goal position $\boldsymbol{X}_e = (x_e, y_e, z_e)^T$ and orientation $\boldsymbol{\Theta}_e = (\phi_e, \theta_e, \psi_e)^T$ of the end effector. To compute the corresponding robot posture by projection, we define a configuration as follows.

$$\boldsymbol{q}_{goal} = [\boldsymbol{X}_e^T \ \boldsymbol{\Theta}_e^T \ z_w \ \boldsymbol{\Theta}_w^T] \tag{10}$$

This is concatenation of the end-effector position and orientation $\boldsymbol{X}_e$, $\boldsymbol{\Theta}_e$, the height of the waist z_w and an orientation of the waist base $\boldsymbol{\Theta}_w = (\phi_w, \theta_w, \psi_w)^T$. A sampled $\boldsymbol{q}_{goal}$ is projected so that it does not violate the stability and kinematic constraints, assuming that:

1. the whole mass concentrates on a point fixed to the waist at $\boldsymbol{COM}_{approx}$ as shown in Fig. 10.
2. the arms and legs are composed of six DOFs. This is the case of our humanoid robot, HRP-2 [20].

First, based on this assumption 1, we can determine the waist horizontal position easily so that $\boldsymbol{COM}_{approx}$ does not move. This can be done by computing the

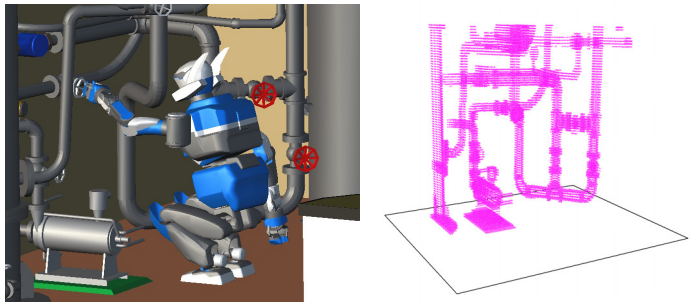

(a) (b)

Fig. 9 Example of a task in complex plant environment: (a) the reaching task to manipulate the valve (b) point cloud representation of the environment based on laser measurement.

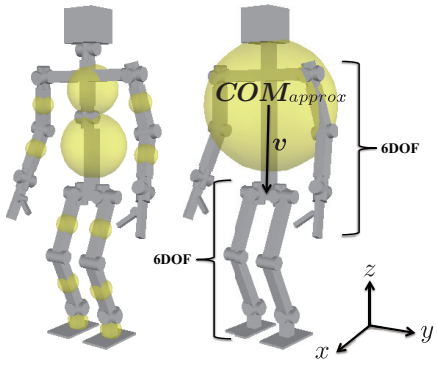

Fig. 10 The original kinematic chain(left) and the simplified kinematic chain used to find goal postures(right). Some of joints are fixed and the original kinematic chain is split into four 6DOF chains connected through the waist. Distributing masses are assumed to be concentrating on the waist.

waist base position $\boldsymbol{X}_w$ from $\boldsymbol{COM}_{approx}$ based on a fixed relative vector $\boldsymbol{v}$ from $\boldsymbol{COM}_{approx}$ to the origin of the waist link, its sampled orientation $\boldsymbol{\Theta}_w$ and height z_w.

Then from this waist base position, angles of the arms are computed by solving analytical solutions of inverse kinematics using the waist position and orientation $\boldsymbol{X}_w$, $\boldsymbol{\Theta}_w$ and end-effector position and orientation $\boldsymbol{X}_e$, $\boldsymbol{\Theta}_e$. The joint angles of legs are calculated to keep the feet positions in the same way. We have verified that the error of approximation of COM is Within 2cm in most of the cases [18] and those errors are compensated during the execution time.

A reaching motion is planned using RRT-Connect [26]. The initial configuration and goals obtained by the projection are used as goals for search trees. For the reaching motion planning as well, only analytical solution of inverse kinematics is used to find solutions quickly. The configuration space for reaching motions is defined as follows:

$$\boldsymbol{q}_{plan} = [\boldsymbol{q}_{arm}^T \; z_w \; \boldsymbol{\Theta}_w^T] \tag{11}$$

where $\boldsymbol{q}_{arm}$ is an array of joint angles of an arm used to reach. While RRT-Connect grows a tree, the horizontal position of the waist base is determined in the same way the projection described above to keep the robot balance. Leg joint angles are computed by solving analytical solution of inverse kinematics as well.

In addition to the one-shot motion planning [18], reactive path replanning [56, 52] is performed in case of there are (possibly unknown) moving obstacles that are also measured as voxels or point clouds represented as sphere tree here. Assuming that all this point information comes from sensors, we actually do not have to distinguish static and moving obstacles, but we just need to update the newly measured

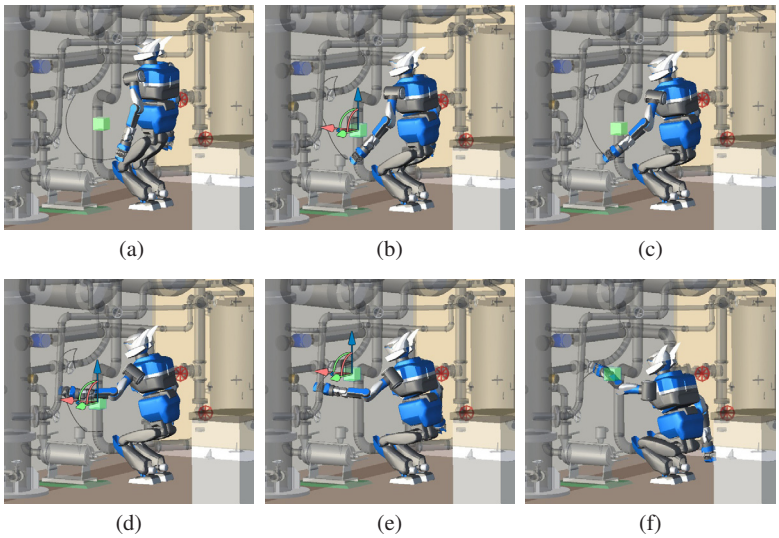

Fig. 11 Reaching motion replanned to avoid a moving obstacle in a complex environment

region. The whole environment of 4m x 5m is represented by around 25,000 points like Fig. 9b with the resolution of 2 cm which are modeled as spheres of radius 1 cm. The average time required for sphere-tree model reconstruction was 28.3 ms on average with Intel(R) processor Core(TM) i7 CPU with 2.70GHz. Although an optimal data management is preferable in case of partial changes, collision model updating is not a bottleneck in this scale of environment.

Figure 11 shows snapshots of replanning process to a valve in a plant environment, where the obstacles are displayed as transparent for better visibility. The green cube simulates an unknown or moving obstacle that is detected only when the robot gets closer to the goal. A collision-free path of reaching with the left hand is first planned as shown in Fig. 11a. When the obstacle moves downwards, new path is immediately replanned by avoiding outside (Fig. 11b, c). The obstacle finally comes upwards, which leads the replanned path to avoid underneath (Fig. 11d, e).

The whole-body motion planning described so far can be utilized for a teleoperated humanoid to ensure minimum autonomy that can interpret and execute commands from an operator. In this case, the operator may want to give commands with certain abstraction level like “reach that point” or “rotate that valve”, to perform motions like in Fig. 11, from a mobile or tablet interface from a distant place where the operator cannot see the robot directly. In DARPA Robotics Challenge (DRC) [6], several manipulation tasks are required such as door opening, turning valves, making a hole on the wall with tools, pushing a button and plugging a socket. The difficulty lies in the variance of tasks whose parameters like the valve diameter or manipulation positions are changed over time. The robot should perform measurements in the world to localize and to recognize the target objects. For the AIST-NEDO team that participated in DRC, the presented whole-body motion planning in this section was integrated a graphical user interface (GUI) based on Choreonoid humanoid simulation framework [34] to execute the manipulation tasks [35] as shown in Fig. 12.

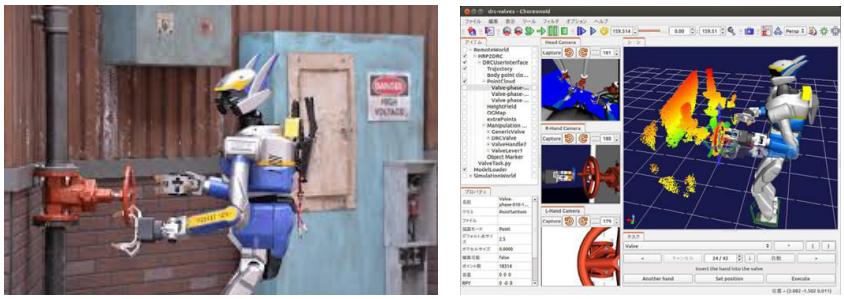

Fig. 12 HRP-2 humanoid robot of AIST-NEDO team executing the valve turning task, and its teleoperation GUI on Choreonoid during DARPA Robotics Challenge.

3.3 Applications: Footstep Planning and Whole-body Manipulation

The whole-body motion planning combining global planning and local motion generation can be extended to more complex applications including stepping and manipulation.

One extension particular to humanoid is incorporating stepping in the framework of whole-body generalized inverse kinematics. Kanoun et al. [23] introduced an augmented robot structure by introducing "virtual" planar links attached to a foot that represents footsteps as illustrated in Fig. 13. This modeling makes it possible to solve the footstep planning as a problem of inverse kinematics, and also to determine the final whole-body configuration. Collision avoidance or balance constraints can be integrated as inequality tasks in the whole-body motion generation introduced as eqs. (6) - (9). After planning the footsteps, the dynamically stable whole-body motion including walking can be computed by using the method presented earlier.

Figure 14 shows an experiment of picking up an object from the floor. The objective here is to pick up a small object lying on the ground between the feet of the robot. A classical generalized inverse kinematic method would detect that the object is within reach without locomotion, but the robot would fail in grasping the target due to self-collision. By applying the proposed approach authorizing a few steps, the required stepping is found in a seamless way. To avoid stepping on the object before reaching for it, the footprints are constrained to avoid a virtual obstacle covering the object.

The solution for this scenario which took 0.9s to solve on a 2.13GHz Intel(R) Core(TM)2 CPU. The actual motion where the robot steps over the planned footprints

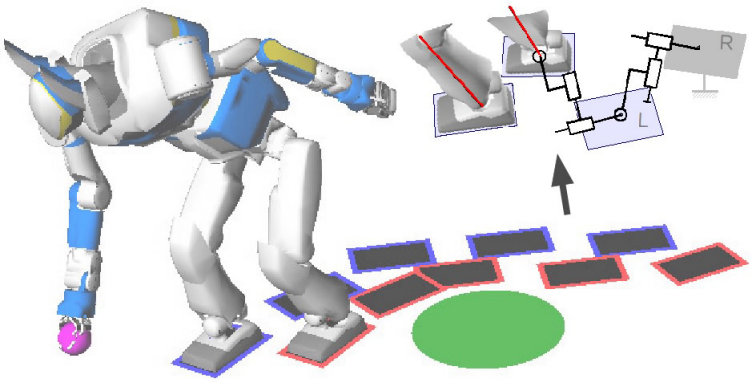

Fig. 13 Footstep planning modeled as a whole-body inverse kinematic problem [23]. Upper left: footsteps are modeled by virtual serial linear and rotational joints attached at the humanoid feet so that generalized inverse kinematics can be directly applied.

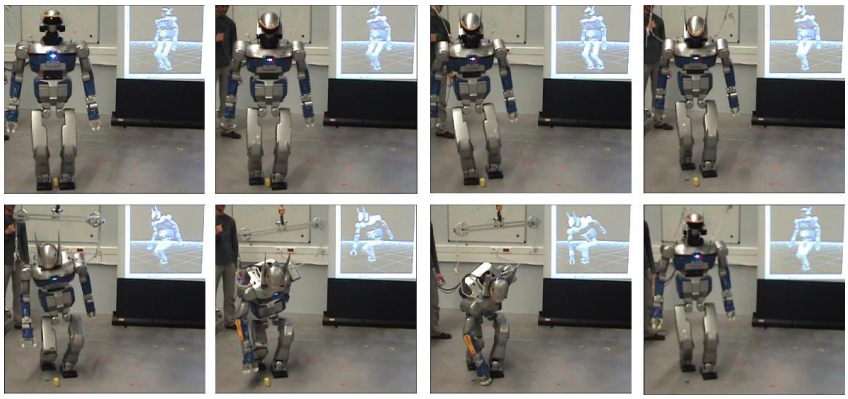

Fig. 14 HRP-2 picking up an object lying between its feet. First a dynamic walk is planned over the support polygons produced by the local foot placement planner, then the whole body is driven by a reaching task while observing self-collision avoidance constraints [23].

was calculated using numerical inverse kinematics with a dynamic stepping pattern generator described by [16]. The coupling between those two frameworks was previously described by [53].

Next application is the manipulation task requiring whole-body motion, which is one of the tasks that are appropriate for humanoid robots. A pioneering study on whole-body manipulation by a humanoid is Harada's research [11, 12] in mid-2000's. The key idea is to control the COM of the robot so that the "static balancing point" is on the center of the foot supporting polygon. The static balancing point is the point to which all the resistance force from both hands and gravity are applied. At the same time, motion planning for humanoid manipulation has also started attracting attention. Stilman proposed a motion planning algorithm for "Navigation Among Movable Obstacles" [45] that allows the humanoid to reach the goal by changing the position of movable objects, whose effectiveness has been experimentally validated later [46].

In the following, we present whole-body motion planning for "pivoting" manipulation that allows displacing a bulky object without lifting it, but by using the contact with the ground. We here model the problem of 3D box pivoting as the problem of pivoting a 2D segment around its endpoints (Fig. 15).

The motion planning algorithm we propose is a two-step approach: first, a collision-free path is computed, and then it is iteratively approximated by a sequence of pivoting motions.

Since we want the robot to walk either forward or backward and to avoid sideways steps, we adopted Reeds and Shepp curves [39], composed of arc of a circle and straight line segments as the first collision-free path, in order to take into account the constraints of the moving direction of a humanoid. In this case we can apply a motion planning technique for a nonholonomic vehicle [27].

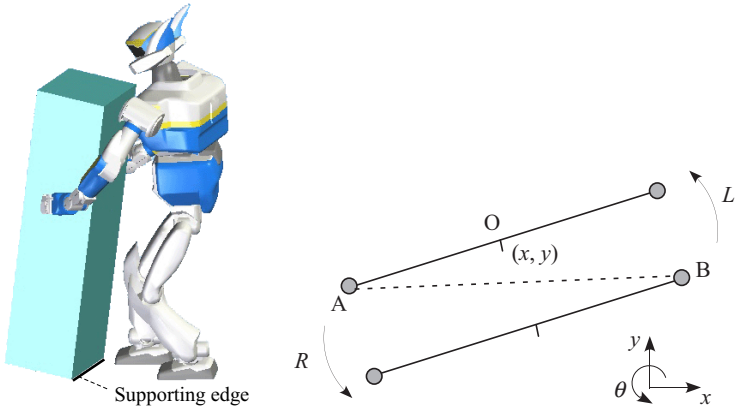

Fig. 15 Supporting edge and pivoting problem modeling. (a) The pivoting sequence is planned using rotation of the endpoints of this edge. (b) The 3D pivoting problem is reduced to how to displace a line segment on vertices A or B.

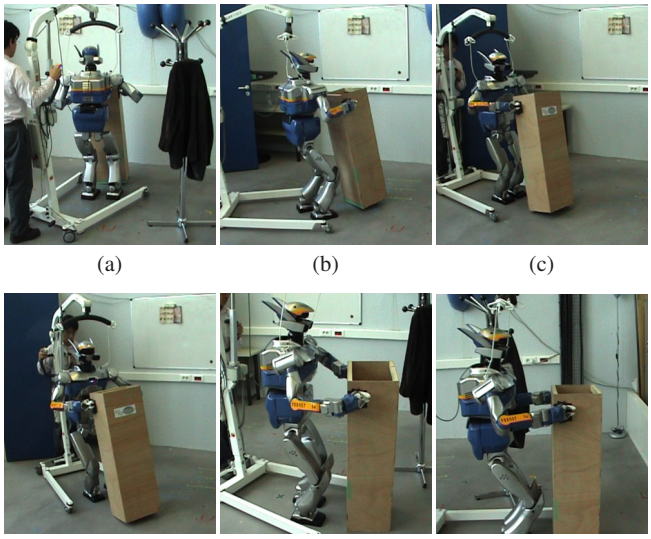

Fig. 16 Experimental results of pivoting manipulation. Starting from the initial position (a) with obstacle at right-hand side, the humanoid robot manipulates the object backwards away from the wall (b). After switching motion direction to forward (c), the robot continues to manipulate the object to the goal position by avoiding the obstacle (d-f).

Then the derived Reeds and Shepp curves are converted into a pivoting sequence. Based on the result by the authors [54] demonstrating the small-time controllability of a pivoting system, the proposed planner is proven to inherit from the probabilistic completeness of the sampling-based motion planning method it is built on.

After the pivoting sequence of the manipulated box is generated, it should be executed by the humanoid robot using its two arms. For this purpose we adopt the dynamic whole-body motion generation in section 3. The task given to the whole-body motion generator is the hand trajectory that is computed from planned box motion.

We have conducted the experiments with the humanoid robot HRP-2 for whole-body motion planning for pivoting of a box-shape object. The experimental results are shown in Fig. 16 to validate the proposed method. The motion has been planned offline with the prior knowledge of the object and environment. The humanoid robot executes the complex pivoting manipulation with a coordinated whole-body motion including simultaneous manipulation and foot-stepping. As can be seen, the robot could accomplish the long pivoting sequence.

As the next step of development, we provide a humanoid robot with more flexibility in whole-body pivoting manipulation by introducing regrasp planning. The robot releases the object when it cannot go further towards the goal position and grasp it again to continue manipulation. We here address the regrasp planning problem for pivoting manipulation through a roadmap-multiplexing approach [55], which is a variant of the method proposed in [44].

Fig. 17 illustrates the overview of the planning scheme. Several grasping positions are possible for a given object position. There are two types of roadmap: the

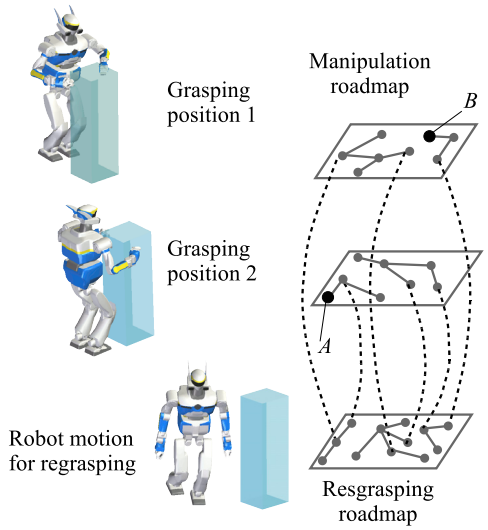

Fig. 17 Roadmap multiplexing. Different manipulation roadmaps are connected by way of the regrasping roadmap at the bottom

first is the "manipulation roadmap" where the robot and the object move together, and the "regrasping roadmap" where the robot moves alone between different grasping positions. As can be seen in the figure, manipulation roadmaps for different grasping positions are interconnected via the regrasping roadmap. For instance, the path from *A* to *B* is possible only by alternating the different grasping positions.

Figure 18 shows the result of regrasp planning. The humanoid robot HRP-2 should carry a box-share object from the initial position (Fig. 18a) to its goal (Fig. 18h). The humanoid robot displaces the object at the entry of a narrow passage (Fig. 18b, c). Then it releases the object and walks to the other side of the wall (Fig. 18d). By combining backward and forward manipulation, the humanoid goes to another narrow passage (Fig. 18e, f). After another regrasping, the object is carried to the goal position (Fig. 18g, h).

Recently Murooka et al. extended the range of whole-body manipulation tasks by a humanoid so that it can select an appropriate way of manipulation from carrying pushing/pulling, and pivoting according to the geometric and physical property of the manipulated object [32].

4 Future Directions and Open Problems

In this chapter, we have introduced whole-body motion planning and generation by efficiently combining sampling-based motion planning and generalized inverse kinematics and dynamic walking pattern generator. We have seen that a variety of

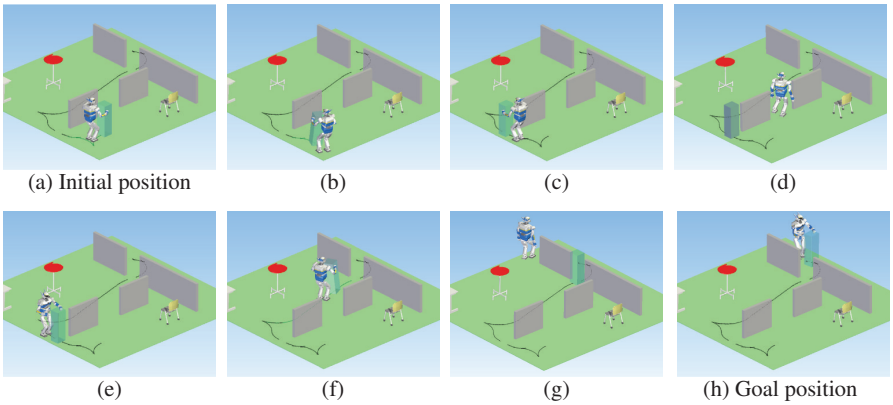

Fig. 18 Simulation result of regrasp planning. Starting from initial position (a), the humanoid robot makes pivoting sequences (b) first puts the object to the entry of passage (c). It leaves the object and walks freely by combining forward and sideways walking (d) to regrasp the object on the other side (e). Then the robot goes towards another narrow passage (f) and makes another regrasp sequence (g) to arrive at the goal (h).

tasks can be performed based on this approach. Next step would be to plan more dynamic motions. Around the year 2000, "kinodynamic motion planning" has already been proposed where dynamic controller is integrated in sampling-based planning [29]. In this work, the planner searches the controller output like velocity, unlike the planning in configuration spaces. This idea has first linked to walking pattern generator taking into account the upper body [13] to plan whole-body collision-free motion and locomotion on rough terrain by supporting the body with the hands contacting the environment.

Optimization-based motion generation based on sequential QP that was utilized to solve generalize inverse kinematics with inequalities in section 3.2 is currently being intensively investigated for dynamic motion control in humanoid research field. This method searches for the optimal sets for the sequence of QPs by minimizing the error to the desired equality tasks in such a way that inequality ones can also be satisfied at a desired priority. This method allows the humanoid to perform such a task of reaching its arm towards an object on the floor without obstructing its view.

This approach based on cascaded QP can be generalized to generate whole-body motions including dynamic equality and inequality tasks [40, 8]. In addition to inverse kinematics considered so far, inverse dynamics is also integrated to the task-priority whole-body motion generation framework. By using this method, the dynamic balance can be addressed directly without converting the dynamic ZMP constraint into COM velocity via a pattern generator. This approach assumes a torque-controlled humanoid as opposed to position controlled ones that are often the case for platform currently used. Dynamic whole-body motion generation with various tasks is being actively studied owing to not only recent progress of robot hardware [37] but also increasing interests on more complex tasks including multiple contacts presented in Chapter **??**. Integration with advanced motion planning techniques with those optimization-based dynamic motion generation is expected to be the key issue for whole-body motion planning for coming several years.

References

1. Baerlocher, P., Boulic, R.: An inverse kinematics architecture enforcing and arbitrary number of strict priority levels. The Visual Computer **20**, 402–417 (2004)
2. Berenson, D., Srinivasa, S., Kuffner, J.: Task space regions: A framework for pose-constrained manipulation planning. Int. J. Robotics Research **30**(12), 1435–1460 (2011)
3. Berenson, D., Srinivasa, S.S., Ferguson, D., Collet, A., Kuffner, J.J.: Manipulation Planning with Workspace Goal Regions. In: Proc. 2009 IEEE Int. Conf. on Robotics and Automation, pp. 1397–1403 (2009)
4. Choset, H., Lynch, K., Hutchinson, S., Kantor, G., Burgard, W., Kavraki, L., Thrun, S.: Principles of Robot Motion: Theory, Algorithms, and Implementation. MIT Press (2006)
5. Dalibard, S., Nakhaei, A., Lamiraux, F., Laumond, J.P.: Whole-body task planning for a humanoid robot: a way to integrate collision avoidance. In: Proc. 2009 IEEE-RAS Int. Conf. on Humanoid Robots, pp. 355 –360 (2009)
6. Defense Advanced Resaerch Projects Agency, "darpa robotics challenge". http://www.theroboticschallenge.org/ (2015)

7. Dubins, L.E.: On curves of minimal length with a constraint on average curvature and prescribed initial and terminal positions and tangents. American Journal of Mathematics **79**, 497–516 (1957)
8. Escande, A., Mansard, N., Wieber, P.B.: Hierarchical quadratic programming: Fast online humanoid-robot motion generation. International Journal of Robotics Research **33**(7), 1006–1028 (2014)
9. Esteves, C., Arechavaleta, G., Pettré, J., Laumond, J.P.: Animation planning for virtual characters cooperation. ACM Trans. on Graphics **25**(2), 319–339 (2006)
10. Gleicher, M.: Comparing constraint-based motion editing method. Graphical Models **63**, 107–134 (2001)
11. Harada, H., Kajita, S., Kanehiro, F., Fujiwara, K., Kaneko, K., Yokoi, K., Hirukawa, H.: Real-time planning of humanoid robot's gait for force controlled manipulation. In: Proc. 2004 IEEE Int. Conf. on Robotics and Automation, pp. 616–622 (2004)
12. Harada, H., Kajita, S., Saito, H., Morisawa, M., Kanehiro, F., Fujiwara, K., Kaneko, K., Hirukawa, H.: A humanoid robot carrying a heavy object. In: Proc. 2005 IEEE Int. Conf. on Robotics and Automation, pp. 1712–1717 (2005)
13. Harada, K., Morisawa, M., Miura, K., Nakaoka, S., Fujiwara, K., Kaneko, K., Kajita, S.: Kinodynamic gait planning for full-body humanoid robots. In: Proc. 2008 IEEE/RSJ Int. Conf. on Intelligent Robots and Systems, pp. 1544–1550 (2008)
14. Hirai, K., Hirose, M., Haikawa, Y., Takenaka, T.: The development of honda humanoid robot. In: Proc. of 1998 IEEE Int. Conf. on Robotics and Automation, pp. 1321–1326 (1998)
15. Hsu, D., Latombe, J.C., Sorkin, S.: Placing a robot manipulator amid obstacles for optimized execution. In: Proc. 1999 Int. Symp. on Assembly and Task Planning, pp. 280–285 (1999)
16. Kajita, S., Kanehiro, F., Kaneko, K., Fujiwara, K., Harada, K., Yokoi, K., Hirukawa, H.: Biped walking pattern generation by using preview control of zero-moment point. In: Proc. 2003 IEEE Int. Conf. on Robotics and Automation, pp. 1620–1626 (2003)
17. Kajita, S., Kanehiro, F., Kaneko, K., Fujiwara, K., Harada, K., Yokoi, K., Hirukawa, H.: Resolved momentum control: Humanoid motion planning based on the linear and angular momentum. In: Proc. 2003 IEEE/RSJ Int. Conf. on Intelligent Robots and Systems, pp. 1644–1650 (2003)
18. Kanehiro, F., Yoshida, E., Yokoi, K.: Efficient reaching motion planning and execution for exploration by humanoid robots. In: Proc. 2012 IEEE/RSJ Int. Conf. on Intelligent Robots and Systems, pp. 1911–1916 (2012)
19. Kanehiro, F., Yoshida, E., Yokoi, K.: Efficient reaching motion planning method for low-level autonomy of teleoperated humanoid robots. Advanced Robotics **28**(7), 433439 (2014). DOI 10.1080/01691864.2013.876931
20. Kaneko, K., Kanehiro, F., Kajita, S., Hirukawa, H., Kawasaki, T., M. Hirata, K.A., Isozumi, T.: The humanoid robot HRP-2. In: Proc. 2004 IEEE Int. Conf. on Robotics and Automation, pp. 1083–1090 (2004)
21. Kanoun, O., Lamiraux, F., Wieber, P.B.: Kinematic control of redundant manipulators: Generalizing the task priority framework. IEEE Transactions on Robotics **27**(4), 785–792 (2011)
22. Kanoun, O., Lamiraux, F., Wieber, P.B., Kanehiro, F., Yoshida, E., Laumond, J.P.: Prioritizing linear equality and inequality systems: application to local motion planning for redundant robots. In: Proc. 2009 IEEE Int. Conf. on Robotics and Automation, pp. 2939–2944 (2009)
23. Kanoun, O., Laumond, J.P., Yoshida, E.: Planning foot placements for a humanoid robot: a problem of inverse kinematics. International Journal of Robotics Research **30**(4), 476–485 (2011). DOI 10.1177/0278364910368147
24. Kavraki, L., Svestka, P., Latombe, J.C., Overmars, M.: Probabilistic roadmaps for path planning in high-dimensional configuration spaces. IEEE Trans. on Robotics and Automation **12**(4), 566–580 (1996)
25. Kuffner, J., Kagami, S., Nishiwaki, K., Inaba, M., Inoue, H.: Dynamically-stable motion planning for humanoid robots. Autonomous Robots **12**(1), 105–118 (2002)
26. Kuffner, J., LaValle, S.: RRT-connect: An efficient approach to single-query path planning. In: Proc. 2004 IEEE Int. Conf. on Robotics and Automation, pp. 995–1001 (2004)

27. Laumond, J.P. (ed.): Robot Motion Planning and Control, *Lectures Notes in Control and Information Sciences*, vol. 229. Springer (1998)
28. LaValle, S.: Planning Algorithm. Cambridge University Press (2006)
29. LaValle, S., Kuffner, J.: Randomized kinodynamic planning. In: Proc. 1999 IEEE Int. Conf. on Roboics and Automation, pp. 473–479 (1999)
30. LaValle, S., Kuffner, J.: Rapidly-exploring random trees: Progress and prospects. In: K.M. Lynch, D. Rus (eds.) Algorithmic and Computational Robotics: New Directions, pp. 293–308. A K Peters (2001)
31. Mansard, N., Stasse, O., Chaumette, F., Yokoi, K.: Visually-guided grasping while walking on a humanoid robot. In: Proc. 2007 IEEE Int. Conf. on Robotics and Automation, pp. 3042–3047 (2007)
32. Murooka, M., Noda, S., Nozawa, S., Kakiuchi, Y., Okada, K., Inaba, M.: Manipulation strategy decision and execution based on strategy proving operation for carrying large and heavy objects. In: Proc. of 2014 IEEE Int. Conf. on Robotics and Automation, pp. 3425–3432 (2014)
33. Nakamura, Y.: Advanced Robotics: Redundancy and Optimization. Addison-Wesley Longman Publishing, Boston (1991)
34. Nakaoka, S.: Choreonoid: Extensible virtual robot environment built on an integrated gui framework. In: Proc. 2012 IEEE/SICE International Symposium on System Integration, pp. 79–85 (2012)
35. Nakaoka, S., Morisawa, M., Cisneros, R., Sakaguchi, T., Kajita, S., Kaneko, K., Kanehiro, F.: Task sequencer integrated into a teleoperation interface for biped humanoid robots. In: Proc. 2015 IEEE-RAS Int. Conf. on Humanoid Robots, pp. 895–900 (2015)
36. Okada, K., Kojima, M., Sagawa, Y., Ichino, T., Sato, K., Inaba, M.: Vision based behavior verification system of humanoid robot for daily environment tasks. In: Proc. 2006 IEEE-RAS Int. Conf. on Humanoid Robots, pp. 7–12 (2006)
37. Ott, C., Baumgrtner, C., Mayr, J., Fuchs, M., Burger, R., Lee, D., Eiberger, O., Albu-Schffer, A., Grebenstein, M., Hirzinger, G.: Development of a biped robot with torque controlled joints. In: Proc. 2010 IEEE-RAS Int. Conf. on Humanoid Robots, pp. 167–173 (2010)
38. Quinlan, S.: Efficient distance computation between non-convex objects. In: Proc. 1994 IEEE Int. Conf. on Robotics and Automation, pp. 3324–3329 (1994)
39. Reeds, J.A., Shepp, R.A.: Optimal paths for a car that goes both forwards and backwards. Pacific Journal of Mathematics **145**(2), 367–393 (1990)
40. Saab, L., Mansard, N., Keith, F., Fourquet, J.Y., Soueres, P.: Generation of dynamic motion for anthropomorphic systems under prioritized equality and inequality constraints. In: Proc. of 2011 IEEE Int. Conf. on Robotics and Automation, pp. 1091–1096 (2011)
41. Sentis, L., Khatib, O.: Synthesis of whole-body behaviors through hierarchical control of behavioral primitives. Int. J. of Humanoid Robotics **2**(4), 505–518 (2005)
42. Sian, N.E., Yokoi, K., Kajita, S., Tanie, K.: A framework for remote execution of whole body motions for humanoid robots. In: Proc. 2004 IEEE/RAS Int. Conf. on Humanoid Robots, pp. 608–626 (2004)
43. Siciliano, B., Slotine, J.J.E.: A general framework for managing multiple tasks in highly redundant robotic systems. In: Proc. IEEE Int. Conf. on Advanced Robotics, pp. 1211–1216 (1991)
44. Simeon, T., Laumond, J.P., Cortes, J., Sahbani, A.: Manipulation planning with probabilistic roadmaps. Int. J. of Robotics Research **23**(7-8), 729–746 (2004)
45. Stilman, M., Kuffner, J.: Navigation among movable obstacles: Real-time reasoning in complex environments. In: Proc. 2004 IEEE-RAS Int. Conf. on Humanoid Robotics, pp. 322 – 341 (2004)
46. Stilman, M., Nishiwaki, K., Kagami, S., Kuffner, J.: Planning and executing navigation among movable obstacles. In: Proc. 2006 IEEE/RSJ Int. Conf. on Intelligent Robots and Systems, pp. 820 – 826 (2006)
47. Sugiura, H., Gienger, M., Janssen, H., Goerick, C.: Real-time collision avoidance with whole body motion control for humanoid robots. In: Proc. 2004 IEEE/RSJ Int. Conf. on Intelligent Robots and Systems, pp. 2053–2058 (2007)

48. Suleiman, W., Yoshida, E., Kanehiro, F., Laumond, J.P., Monin, A.: On human motion imitation by humanoid robot. In: Proc. 2008 IEEE Int Conf. Robotics and Automation, pp. 2697–2704 (2008)
49. Suleiman, W., Yoshida, E., Laumond, J.P., Monin, A.: On humanoid motion optimization. In: Proceedings of 7th IEEE-RAS International Conference on Humanoid Robots, pp. 180–187 (2007)
50. Weghe, M.V., Ferguson, D., Srinivasa, S.S.: Randomized path planning for redundant manipulators without inverse kinematics. In: Proc. 2007 IEEE-RAS Int. Conf. on Humanoid Robots, pp. 477–482 (2007)
51. Yoshida, E., Esteves, C., Belousov, I., Laumond, J.P., Sakaguchi, T., Yokoi, K.: Planning 3D collision-free dynamic robotic motion through iterative reshaping. IEEE Trans. on Robotics **24**(5), 1186–1198 (2008). DOI 10.1109/TRO.2008.2002312
52. Yoshida, E., Kanehiro, F.: Reactive robot motion using path replanning and deformation. In: Proc. 2011 IEEE Int. Conf. on Robotics and Automation, pp. 5457–5462 (2011)
53. Yoshida, E., Kanoun, O., Esteves, C., Laumond, J.P., Yokoi, K.: Task-driven support polygon reshaping for humanoids. In: Proceedings of 6th IEEE-RAS International Conference on Humanoid Robots, pp. 827–832 (2006)
54. Yoshida, E., Poirier, M., Laumond, J.P., Alami, R., Yokoi, K.: Pivoting based manipulation by humanoids: a controllability analysis. In: Proc. 2007 IEEE/RSJ Int. Conf. on Intelligent Robots and Systems, pp. 1130–1135 (2007)
55. Yoshida, E., Poirier, M., Laumond, J.P., Kanoun, O., Lamiraux, F., Alami, R., Yokoi, K.: Regrasp planning for pivoting manipulation by a humanoid robot. In: Proc. 2009 IEEE Int. Conf. on Robotics and Automation, pp. 2467–2472 (2009)
56. Yoshida, E., Yokoi, K., Gergondet, P.: Online replanning for reactive robot motion: Practical aspects. In: Proc. 2010 IEEE/RSJ Int. Conf. on Intelligent Robots and Systems, pp. 5927–5933 (2010)
57. Yoshikawa, T.: Manipulability of robotic mechanisms. Int. J. Robotics Research **4**(2), 3–9 (1985)
58. Zacharias, F., Borst, C., Hirzinger, G.: Capturing robot workspace structure: Representing robot capabilities. In: Proc. 2007 IEEE/RSJ Int. Conf. on Intelligent Robots and Systems, pp. 3229–3236 (2007)
59. Zacharias, F., Sepp, W., Borst, C., Hirzinger, G.: Using a model of the reachable workspace to position mobile manipulators for ”3-d” trajectories. In: Proc. 2009 IEEE-RAS Int. Conf. on Humanoid Robots, pp. 55–61 (2009)